Functional Expression Cloning and Characterization of SFT, a Stimulator of Fe Transport

Jesus A. Gutierrez, Jianming Yu, Susan Rivera, and Marianne Wessling-Resnick

Department of Nutrition, Harvard School of Public Health, Boston, Massachusetts 02115

Abstract. A stimulator of Fe transport (SFT) was identified by functional expression cloning in *Xenopus* oocytes. SFT-mediated transport has properties defined for transferrin-independent Fe uptake, but its cytolocalization in recycling endosomes and the observed stimulation of transferrin-bound Fe assimilation indicate a key role in intracellular Fe membrane transport as well. SFT has six predicted transmembranous domains and a functionally important RExxE motif that resembles domains involved in yeast Fe transport and Fe-binding by ferritin L-chains. The observation that SFT oligomerizes, along with other structural and mechanical features, suggests it may be a member of either the ATP-binding cassette or cation diffusion facilitator families. The 3′ untranslated region of SFT contains a translation inhibitory element and inhibition of SFT expression in *Xenopus* oocytes was found to be relieved by coinjection of transcripts from other defined cDNAs that are also described in this report. SFT is the first component of the mammalian Fe membrane transport machinery to be identified.

IRON is absolutely essential to sustain life and maintain growth of mammalian cells. Much of the iron delivered to cells enters mitochondria where heme is synthesized for incorporation into mitochondrial cytochromes, extramitochondrial cytochromes (e.g., P450), or key functional proteins (e.g., hemoglobin and myoglobin). Iron is also necessary for nonheme factors (e.g., Fe-S proteins) and Fe-requiring enzymes (e.g., ribonucleotide reductase). Additionally, all cells contain ferritin that serves as a storage depot; levels of the protein reflect cellular iron status due to this function.

Despite our fundamental knowledge of the use and storage of this key nutrient, relatively little is known about the translocation of Fe across biological membranes. Iron is typically acquired by mammalian cells through receptor-mediated endocytosis of transferrin (Tf).[1] Internalized diferric Tf is delivered to endosomes where Fe is released due to the low pH of this compartment (Dautry-Varsat et al., 1983; Klausner et al., 1983), yet exactly how the cation is subsequently transferred to the cytosol and mitochondria to fulfill its critical metabolic functions remains unclear. Iron transport across endosomal membranes is thought to involve the reduction of Fe^{3+} to Fe^{2+} (Nunez et al., 1990; Watkins et al., 1992; Oshiro et al., 1993) but the Fe-translocating machinery has yet to be defined. Cells can also translocate non–Tf-bound Fe across the plasma membrane (Sturrock et al., 1990; Inman and Wessling-Resnick, 1993); in fact, this process may play an important role in pathologic states such as hemochromatosis wherein Tf reaches saturation. The characteristics of Tf-independent transport also suggest a role for a ferrireductase activity (Inman et al., 1994; Jordan and Kaplan, 1994; Randell et al., 1994; Riedel et al., 1995), but the relationship between cell surface and endosomal Fe membrane carriers is unknown. Functionally, the role for a ferrioxidoreductase in Fe membrane transport is compatible with mechanistic features of yeast (Dancis et al., 1992; Askwith et al., 1994; Dix et al., 1994; De Silva et al., 1995; Stearman et al., 1996) and plant (Eide et al., 1996) uptake systems, but genetic studies have yet to reveal how translocation of the cation across the bilayer is actually accomplished.

The identification of the membrane components responsible for the bilayer translocation of Fe using biochemical reconstitution approaches has been hampered by its physiochemical properties. Although biologically active Fe^{3+} and Fe^{2+} are both relatively soluble under acidic conditions, at neutral pH under atmospheric conditions, spontaneous oxidation produces insoluble polymeric aggre-

1. *Abbreviations used in this paper*: ABC, ATP-binding cassette; ACADM, acyl co-A dehydrogenase; GFP, green fluorescent protein; NTA, nitrilo-acetic acid; ORF, open reading frame; PMA, phorbol 12-myristate 13-acetate; SFT, stimulator of Fe transport; Tf, transferrin; TIE, translation inhibitory element; UTR, untranslated region; XFGFR, *Xenopus* FGF receptor.

gates of $Fe(OH)_3$. A second very dangerous consequence is Fenton chemistry elicited from Fe^{2+} to produce hydroxyl radicals capable of damaging biological molecules at a diffusion-controlled rate. To counter these problems, Fe rarely exists freely in biological systems; instead, the cation is associated with proteins, like transferrin or lactoferrin, or complexed with low molecular weight chelators, such as citrate or ATP. Most importantly, Fe bioavailability appears to be tightly regulated by mammalian cells through translational control of Tf receptor and ferritin synthesis (for review see Klausner et al., 1993).

Because of the inherent difficulties associated with reconstitution of Fe transport systems, we sought to identify the membrane protein(s) involved by functional expression through microinjection of *Xenopus* oocytes. Here we report the identification and characterization of a human cDNA encoding an integral membrane protein called SFT for stimulator of Fe transport. Transport properties associated with SFT-mediated uptake resemble those defined for non–Tf-bound Fe uptake by K562 cells (Inman and Wessling-Resnick, 1993). Moreover, a green fluorescent protein (GFP) chimera expressed in mammalian cells resides in juxtanuclear recycling endosomes, indicating a role for SFT in Tf-mediated iron delivery. This idea is strongly supported by the observed stimulation of Fe assimilation from Tf. Structural features of the molecule provide some insight into possible transport mechanism(s) for the translocation of Fe across membrane bilayers. Finally, a translational control element related to the translation inhibitory element (TIE) of *Xenopus* fibroblast growth factor (FGF) receptor (XFGFR) mRNA (Robbie et al., 1995) was identified. Translational inhibition of SFT in oocytes was relieved by coinjection of transcripts from other defined cDNAs that are also described here.

Materials and Methods

Microinjection of Xenopus Oocytes and Measurement of Expressed Fe Uptake

Oocyte-positive *Xenopus* females were obtained from Nasco (Fort Atkinson, WI) and maintained at 19°C. Manually defolliculated stage VI oocytes were isolated and allowed to recover overnight in modified Barth's saline supplemented with 2.5 mM sodium pyruvate, penicillin (100 U/ml), and streptomycin (100 μg/ml). The oocytes were injected with either 35 nl water (control) or 35 nl containing either mRNA collected from K562 cells or cRNA transcribed in vitro from pools of the K562 cell library described below. During initial screening, 40 ng cRNA was injected per oocyte, but for final screening experiments and functional characterization, 4–15 ng was injected. To allow expression of transport activity, injected oocytes were incubated 48 h in 70% Leibovitz's L15 media supplemented with 10 mM Hepes, pH 7.5. It should be noted that prolonged incubation periods (>3 d) resulted in death of SFT-injected oocytes, possibly due to Fe toxicity since water-injected oocytes remained viable during this time. For some experiments, oocytes were incubated in Barth's saline containing 1 μM progesterone for 24 h before iron uptake assays.

Fe uptake was measured essentially as described by Inman and Wessling-Resnick (1993), except that oocytes were incubated in 1 μM ^{55}Fe-nitriloacetic acid (NTA) at room temperature for indicated periods of time. Briefly, oocytes were resuspended in 25 mM Hepes, 150 mM NaCl containing 1 mg/ml dextrose, and ^{55}Fe-nitriloacetic acid (1:4 complex) was added. Uptake was quenched upon a 30-min incubation on ice with unlabeled 50 μM FeNTA to remove any externally bound radioisotope; oocytes were then filtered onto nitrocellulose discs and cell-associated radioactivity was determined by scintillation counting. Background measurements determined at 4°C were subtracted.

Construction of cDNA Library, In Vitro Transcription and Screening

K562 cells were treated overnight with 50 nM phorbol 12-myristate 13-acetate (PMA) (Akompong et al., 1995) and polyadenylated (poly[A]) mRNA was isolated to prepare a directional cDNA library in pBSK(−). Avian myeloblastosis virus reverse transcriptase was used for first strand synthesis with a NotI-oligo dT–primer adaptor (Promega Corp., Madison, WI). Second-strand replacement synthesis was immediately carried out using DNA polymerase I and RNase H as described by Gubler and Hoffman (1983). The resulting cDNA was treated with T4 DNA polymerase to flush the ends, and EcoRI adaptors (Promega Corp.) were ligated using T4 DNA ligase. The cDNA was then digested with NotI and phosphorylated with T4 polynucleotide kinase before ligation with NotI/EcoRI-digested pBSK (−). Recombinant plasmids were transformed into XL1-Blue cells (Stratagene, La Jolla, CA) using the procedure of Hanahan (1983). The resulting library was amplified and stored in 15% glycerol at −80°C.

Capped cRNAs were synthesized from the cDNA library in vitro using T7 RNA polymerase in the presence of m^{7}GpppG (Melton et al., 1984). Initial screening of ~40,000 cDNAs indicated that Fe transport activity could be measured upon injection of transcripts, however this signal was unreliably detected upon further rounds of subfractionation of the library. Therefore, an expression cloning strategy was adopted based on the so-called Latin square experimental design (Steel and Torrie, 1980). *Escherichia coli* bearing recombinant plasmids were plated onto 25 plates to form a 5 × 5 matrix, and colonies were scraped into 5 ml Luria-Bertani LB media. A 1-ml aliquot per plate was made to 15% glycerol and stored at −80°C for further analysis. Plasmid DNA was isolated from the remaining sample using the alkaline lysis method described by Birnboim and Dolly (1979). Plasmids from selected plates across each row and column of the 5 × 5 matrix were individually mixed such that 25 "double groupings" were created. The combined plasmids were then linearized by digestion with NotI and capped cRNAs were prepared. The resulting transcripts were injected into five oocytes that were individually assayed for transport activity.

In theory, plates containing individual positive clones should be identified across a given row or column by five replicate samples in the Latin square. However, as described in Results, clones from two independent pools were found to provide transport function only when mixed together in this double-grouping matrix. Holding one group of cRNAs constant, the other set of clones was screened for the ability to stimulate Fe uptake using more conventional iterative panning techniques (Masu et al., 1987). Once a single unique cDNA was isolated, its transcripts were then coinjected with the second pool, which was iteratively panned to isolate four complementing clone(s). Dideoxy chain termination sequencing was performed using forward-advancing primers for both DNA strands and sequence assembly, alignments, and nucleotide and amino acid analyses (FASTA and BLAST) were performed using Genetics Computer Group (Madison, WI) software.

Northern Analysis

K562 cell RNA (40 μg) was electrophoresed on 1% formaldehyde–agarose gels and transferred to nylon membranes as previously described (Akompong et al., 1995). A multiple-tissue Northern blot was obtained from Clontech (Palo Alto, CA). Probes were ^{32}P labeled by random priming; hybridization was at 42°C in 50% formamide containing 5× Denhardt's solution. The blots were washed in 15 mM NaCl, 1.5 mM sodium citrate buffer (0.1× standard sodium chloride–sodium citrate) containing 0.5% SDS at 55°C. Autoradiography was for 5 d at −80°C using intensifying screens.

Subcloning of SFT–Open Reading Frame (ORF) and In Vitro Translation

The predicted SFT-ORF (see Fig. 3) was amplified by PCR with oligonucleotides 5′-GCCATGGGATCCTAAAGAATTTAATCATTGG-3′ and 5′-GCGCTCTAGACAAGGGAGAC-3′ as primers under the following conditions: 5 min at 94°C, 5 min at 72°C, followed by 25 cycles for 45 s at 94°C, 45 s at 55°C, and 1 min at 72°C. A 1.1-kb fragment was generated and after restriction digestion with XbaI and BamHI, the product was directionally subcloned into pAGA, a transcription-competent vector derived from pGEM3Zf(−) with 5′ untranslated sequences of alfalfa mosaic virus RNA-4 and a 3′ stretch of 92 nucleotides such that transcripts incor-

porate a poly(A) tail (Sanford et al., 1991). SFT-ORF was inserted into the cloning cassette of pAGA such that the ATG of the ORF for the alfalfa mosaic virus RNA became the initiation codon. Transcripts were prepared from pAGA-SFT linearized with HindIII using T7 polymerase while full-length SFT transcripts were prepared from pBSK(−) as noted above except that neither were capped. Both transcripts were added to reticulocyte lysate at a concentration of 100 μg/ml with the lysate composing 70% (vol/vol) of the translation mixture, which also included two equivalents of canine microsomal membranes (Promega Corp.). Incubations were at 30°C for 30 min in the presence of 20 μM amino acids minus methionine with $1–2 \times 10^5$ cpm/μl [^{35}S]methionine (Dupont-NEN, Boston, MA) added. After the addition of 50 μg/ml RNase A, samples were denatured in Laemmli sample buffer containing 2.5% β-mercaptoethanol and 1% SDS and were analyzed by SDS-PAGE.

Construction of SFT(E→A) Mutant

Point mutagenesis to introduce alanine residues in place of Glu[83] and Glu[86] in the RExxE motif of SFT was carried out using sequential PCR steps. Two complementary primers (5′-GTGCAGAGCAATCCATCAT-GCGTTAAAAAAT-3′ and 5′-ATTTTTTAACGCATGGATTGCTCT-GCAC-3′) were designed to introduce the alanine substitutions. PCR was performed using pAGA-SFT as template with these primers and the two primers noted above to amplify the ORF thus generating two products of 300 and 800 bp. The reaction conditions were as follows: 3 min at 94°C, four cycles for 30 s at 94°C, 80 s at 45°C, and 1 min at 72°C, followed by 26 cycles for 30 s at 94°C, 60 s at 56°C, and 1 min at 72°C. These fragments were then isolated and used as templates in a second PCR reaction using only the primers to amplify the ORF with the conditions described above to generate pAGA-SFT. After digestion with XbaI and BamHI, the 1.1-kb product was also directionally subcloned into pAGA exactly as detailed above.

Construction of GFP-SFT Chimera

The plasmid bearing GFP, pGreen Lantern–2 (pGL2), was a gift of Dr. P. Hawley-Nelson (Life Technologies, Gaithersburg, MD). To introduce a NotI restriction site, the SFT ORF was amplified by PCR using pAGA-SFT as a template with a universal T7 primer and the oligonucleotide 5′-AATGGCGGCCGCCTTAATTATCAG-3′ under the following reaction conditions: 5 min at 94°C, 30 cycles for 45 s at 94°C, 1 min at 52°C and 1 min 72°C, and then 10 min at 72°C. The PCR product was digested with EcoRI and NotI, and then subcloned into EcoRI- and NotI-digested pGL2 such that immediately after the terminal coding lysine of SFT, three alanine residues from the pGL2 cloning cassette follow with the GFP sequence in frame.

Transfection and Generation of Stable Cell Lines

HeLa cells were transiently transfected using lipofectamine as the DNA carrier as described by the manufacturer (GIBCO BRL, Gaithersburg, MD). Briefly, semi-confluent cells grown on glass coverslips were incubated with DNA–lipofectamine complexes under serum-free conditions for 5 h, and then the media was replaced with fresh DME containing 10% FBS. After 16–24 h of incubation to allow for expression of SFT, cells were fixed and processed for fluorescence microscopy. Stable cell lines were established under similar conditions, except that pGL2-SFT and pCDNA3.1 (Invitrogen, San Diego, CA) were cotransfected into cells at a molar ratio of 10:1 and cells expressing GFP-SFT were selected for by neomycin resistance by plating in media containing 0.8 mg/ml G418 and clonal lines were isolated by limiting dilution. Stable expression of GFP-SFT by the entire cell population was confirmed by fluorescence microscopy.

Fluorescence Microscopy

HeLa cells were grown on glass cover slips and transiently transfected as described above. Immediately before experiments, typically 1 d after transfection, the cells were incubated with 93 nM Texas red–Tf (Molecular Probes, Inc., Eugene, OR) for 45 min at 37°C. Cells were then washed with ice-cold PBS containing 1 mM $MgCl_2$ and 0.1 mM $CaCl_2$, and then fixed with 3% paraformaldehyde in PBS. After quenching with 50 mM NH_4Cl in PBS, cells on the cover slips were rinsed once briefly with water, and then allowed to air dry. Cover slips were mounted using fluormount-G (Southern Biotechnology Associates Inc., Birmingham, AL) containing 2.5 mg/ml N-propyl gallate. Fluorescence microscopy was performed us-

ing an Axioskop epifluorescence microscope (Carl Zeiss, Thornwood, NY) at a nominal magnification of ×100.

Transferrin-bound Iron Uptake Assays

Accumulation of ^{55}Fe from Tf was measured as previously described (Inman and Wessling-Resnick, 1990). Briefly, apoTf (Boehringer-Mannheim Corp., Indianapolis, IN) was incubated with 50-fold excess of ^{55}FeNTA prepared at a molar ratio of 1:2 in PBS containing 10 mM $NaHCO_3$ for 60 min at room temperature. To remove unbound radioactivity, the reaction mixture was desalted by gel filtration using Biogel P6 (Bio-Rad, Hercules, CA); fractions were assayed for protein content and iron saturation (∼1.6 Fe atoms per Tf).

For uptake experiments, HeLa cells were grown in six-well plates to ∼70% confluence and 40 nM [^{55}Fe]Tf was added directly to the 37°C media. At indicated times, uptake was quenched by washing the cells with ice-cold PBS followed by a 45-min incubation on ice with 1 μM unlabeled Tf to remove surface-bound radioactivity. After three washes with ice-cold PBS, cells were harvested in 0.6 ml PBS containing 1 mM EDTA; the number of cells was determined using a hemocytometer and the amount of associated radioactivity was measured by scintillation counting of duplicate 200-μl aliquots.
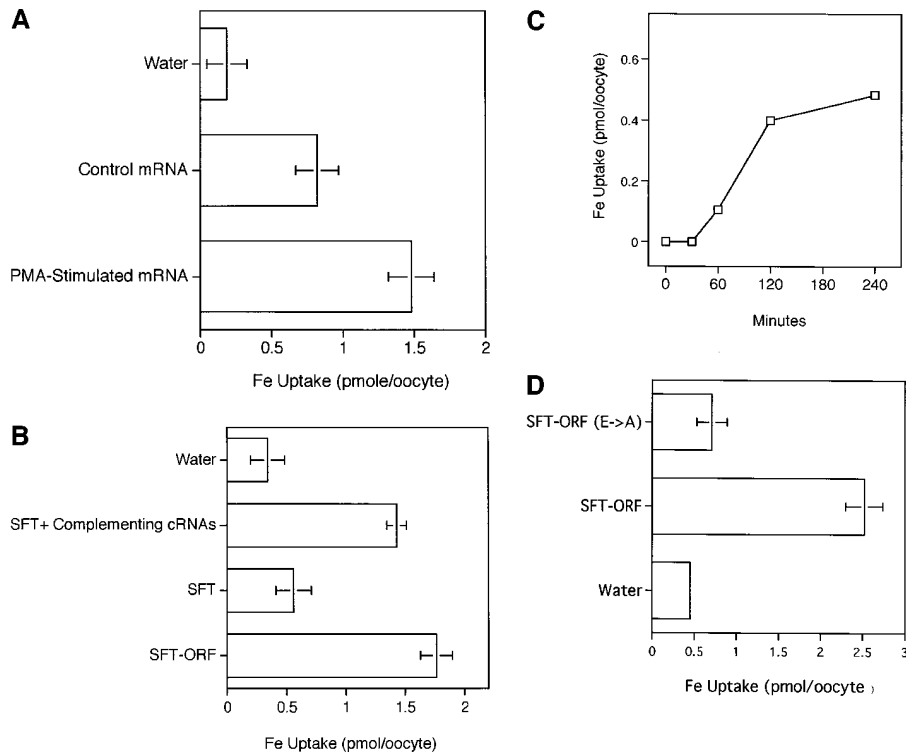
Results

Expression of Exogenous Iron Transport Activity by Xenopus Oocytes

PMA upregulates non–Tf-bound Fe uptake across the plasma membrane of K562 cells by a transcription-dependent mechanism (Akompong et al., 1995). Taking advantage of this observation, efforts were initiated to identify the elements involved in membrane Fe transport by functional expression in Xenopus oocytes. Fig. 1 A demonstrates that upon injection of mRNAs from control and PMA-treated K562 cells, ^{55}Fe uptake by oocytes is stimulated two- and fourfold above background, respectively. Minimal transport activity is detected in control or water-injected cells. Nomizu et al. (1993) have reported that the Fe content of stage VI oocytes remains unchanged during subsequent maturation and fertilization, indicating that Fe uptake is limited with maternal stores providing sufficient Fe throughout early stages of development. Fractionation experiments confirmed the specific Fe transport by injected oocytes, since assimilated ^{55}Fe was incorporated into cytosolic components with <5% of radioactivity associated with membranous components (not shown). Preliminary experiments also revealed that Fe uptake was time and temperature dependent (see below). Thus, expression of Fe transport activity by Xenopus oocytes programmed with K562 cell mRNA bears functional resemblance to the PMA-inducible, Tf-independent Fe carrier previously characterized for K562 cells (Inman and Wessling-Resnick, 1993).

Identification of SFT

In vitro transcripts prepared from a cDNA library established using PMA-induced K562 cell mRNA were also initially found to stimulate Fe uptake when injected into oocytes. To enable identification of positive clones, a double-grouping strategy based on the Latin square experimental design was adopted, as detailed in Materials and Methods. Briefly, the cDNA pool was divided into 25 separate plates to create a 5×5 matrix. Isolated plasmids were then pooled across each row and column of the matrix and in vitro

transcripts were prepared. Activity measurements were carried out by injecting five oocytes with each cRNA mixture and assaying individual cells for Fe uptake activity. Using this approach, cRNAs from two separate but functionally complementing pools of clones were found to stimulate Fe uptake when coinjected. One group of clones was then iteratively panned for activity by coinjecting a fixed set of transcripts from the other complementing pool. A single positive cDNA of ~1,400 bp was identified and because transcripts from this unique clone were necessary to stimulate Fe transport, it was named SFT. Subsequent iterative panning of the second complementing pool by coinjection with the unique SFT transcript yielded four additional cDNAs of ~650, 1,000, 1,400, and 1,900 bp that individually enabled expression of transport activity. Fig. 1 *B* demonstrates that coinjection of SFT with the other cRNAs stimulated oocyte Fe uptake fourfold above background. In contrast, injection of SFT alone stimulated only modest transport activity, whereas injection of the complementing cRNAs either together or individually did not promote Fe uptake above background (not shown). The probable function of the second set of four complementing cRNAs will be discussed later in this report.

As shown in Fig. 2 *A*, Northern analysis of SFT expression in control and PMA-treated K562 cell RNAs reveals the presence of the 1.5- and 2.4-kb transcripts. PMA markedly enhances the level of the 1.5-kb transcript indicating that the SFT cDNA isolated from the PMA-induced K562 cell library must be nearly full length. Human tissue Northern analysis (Fig. 2 *B*) further demonstrates ubiquitous expression of both 1.5- and 2.4-kb transcripts with highest levels observed in peripheral blood leukocytes, spleen, thymus, and small intestine. The latter tissues are known to have enhanced Fe uptake properties, but the ubiquitous pattern of expression suggests that SFT is important for normal cellular function much like Fe transport itself.

Structural Features of SFT

Sequence analysis of the SFT cDNA indicates the insert to be 1,404 bp in length (Fig. 3). The sequence preceding the predicted ATG start codon is consistent with the Kozak consensus translation initiation motif; the fact that 5′ to this ATG there are two in-frame termination codons also supports the idea that SFT contains the entire ORF for a 338–amino acid protein. A polyadenylation signal found within the predicted 3′ UTR is underlined in Fig. 3. The identified primary structure of SFT based on its nucleotide sequence indicates a highly hydrophobic and very basic molecule with 46.2% hydrophobic amino acid composition and a predicted isoelectric point of 10.2. Database searches reveal that SFT is a novel protein with no homology to other reported amino acid sequences, including yeast (Dix et al., 1994; Stearman et al., 1996), plant (Eide et al., 1996), and bacterial (Kammler et al., 1982) Fe transporters.

As shown in Fig. 4 *A*, Kyte-Doolittle analysis (Kyte and Doolittle, 1982) supports the idea that SFT encodes an in-
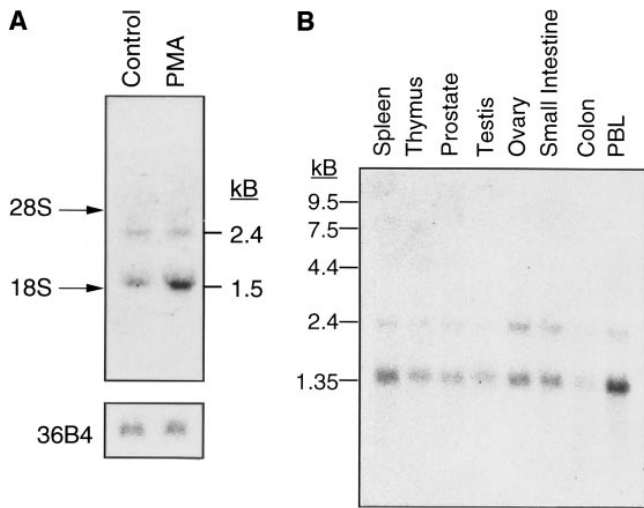
Figure 2. Relative size and abundance of SFT transcripts. (*A*) Total RNA from control or PMA-treated K562 cells was probed with ^{32}P-labeled SFT cDNA under high stringency hybridization conditions. Locations of 28S and 18S ribosomal bands are depicted by left arrows and the approximate molecular sizes for the two transcripts are shown on the right. Equal RNA loading was determined by hybridization with ^{32}P-labeled cDNA for 36B4 ribosomal protein. (*B*) A Northern blot containing 2.5 μg poly(A) RNA from several human tissues was probed with ^{32}P-labeled SFT cDNA. Molecular sizes are depicted on the left.

trinsic membrane protein with at least six transmembrane-spanning domains (M1–M6), which are highlighted in Fig. 3. A hypothetical model of SFT's membrane structure from this analysis is presented in Fig. 4 *B*. Based on the inside-positive rule (Von Hiejne, 1994) and the absence of a clearly defined signal sequence, the NH$_2$ terminus of the protein is tentatively situated on the intracellular face of the membrane. The hypothetical model would then predict that SFT contains a large intracellular loop (L4) and a large extracellular loop (L5), although these domains, Glu^{149}–Met^{224} and His^{246}–Leu^{296}, respectively, also have limited hydrophobic identity. The predicted transmembrane-spanning domains contain several charged amino acids similar to other known ion channels and transporters, however it is particularly noteworthy that M1, M3, and M5 harbor several histidine residues, which are potential ligand sites for metal binding. Finally, a short amino acid stretch in the first predicted cytoplasmic loop, REIHE, resembles functional RExxE motifs previously described for the yeast iron transporter Ftr1 (Stearman et al., 1996) and ferritin L-chains (Trikha et al., 1995).
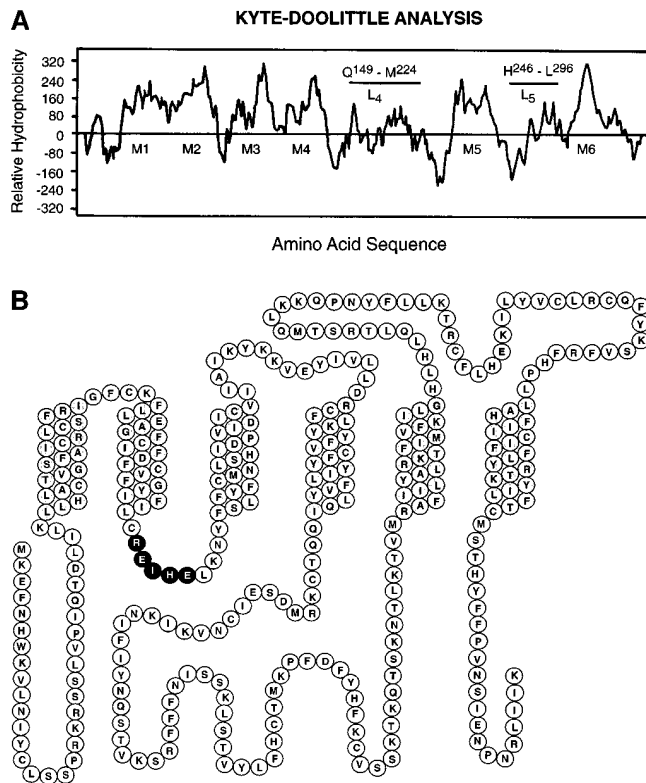
To confirm the predicted ORF, nucleotides 86–1,101 were subcloned into a transcription-competent vector as described in Materials and Methods and in vitro translation experiments using rabbit reticulocyte lysate were performed (Fig. 5). SFT translation required the presence of canine pancreatic microsomes as expected for synthesis of an integral membrane protein. [^{35}S]methionine-labeled products of identical electrophoretic mobility were obtained from transcripts containing the ORF (Fig. 5, lane *B*) and full-length message (Fig. 5, lane *C*), providing direct confirmation of SFT's reading frame. Surprisingly, both products are found to migrate as ∼87-kD species de-
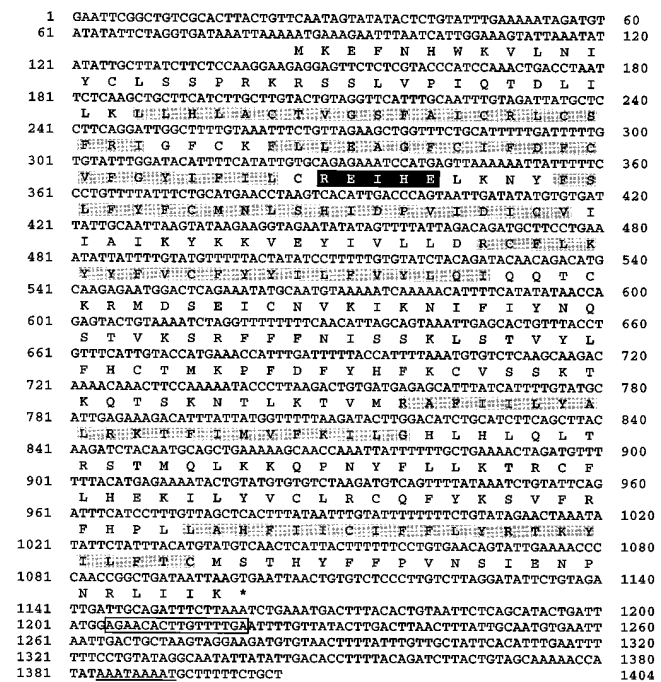
Figure 3. Complementary nucleotide and deduced amino acid sequences of the human SFT cDNA. Nucleotides are numbered in the 5′ to 3′ direction starting with the first base of the cDNA and the deduced single-letter amino acid sequence is shown below beginning with the first methionine. A polyadenylation signal found within the predicted 3′ UTR is underlined. The six putative membrane spanning domains are underlined. The amino acid motif REIHE is indicated in the black box and the predicted transmembrane spanning domains are highlighted. The putative translation inhibitory element is in the open box. Using 5′ and 3′ oligonucleotide primers based on the cDNA coding sequence, a second independent clone was established by RT-PCR amplification of K562 cell mRNA to verify the sequence as shown. These sequence data are available from GenBank/EMBL/DDBJ under accession number AF020761.

spite the fact that a translated product >41 kD can be excluded by the length of in vitro transcripts generated for the subcloned ORF. Treatment with glycanase F did not affect the mobility of the translated products demonstrating that glycosylation does not account for the difference in apparent molecular weight (not shown). The latter result is consistent with the hypothetical model of SFT's membrane structure since N-linked glycosylation sites are absent from the predicted exofacial domains. Thus, SFT appears to homodimerize even in the presence of 2.5% β-mercaptoethanol and 1% SDS.

As shown in Fig. 1 *B*, injection of oocytes with the cRNA encoding the ORF alone is sufficient to stimulate Fe transport in the absence of complementing cRNAs, and this activity was similar to Fe uptake by oocytes coinjected with the full-length SFT cRNA + complementing cRNAs. Transport activity with the defined SFT cRNA (293 ± 22.5 pmol/oocyte/μg) was greatly enhanced relative to that observed upon injection with mRNA from PMA-stimulated cells (74.2 ± 1.5 pmol/oocyte/μg). Moreover, the time course of uptake stimulated by expression of the SFT-ORF alone demonstrates that the accumulation of ^{55}Fe is saturable (Fig. 1 *C*). Thus, it can be concluded that expres-

KYTE-DOOLITTLE ANALYSIS

A

B

Figure 4. Hypothetical model for SFT membrane structure. (*A*) Hydropathy plot of SFT amino acid sequence by Kyte-Doolittle analysis (Kyte and Doolittle, 1982). (*B*) Proposed membrane orientation for SFT from amino acid sequence shown in Fig. 3.

Table I. Fe Transport Inhibition

Inhibitor (concentration)	Percent SFT-mediated Fe uptake
Fe(NH$_4$) Citrate (14.2 mg/ml)	4.4
CdSO$_4$ (20 mM)	24.0
Antimycin A (20 mg/ml)	1.4
Rotenone (1 mM)	2.5

[55]Fe uptake was determined as described for Fig. 1 except that transport assays contained the indicated concentrations of inhibitors ($n = 10$ oocytes). To deplete cellular ATP, oocytes were first exposed to antimycin A or rotenone for 30 min before assays that were then conducted in their presence; ATP levels determined for control, antimycin A and rotenone treated cells were measured to be 11.0 ± 1.7, 5.9 ± 0.9, and 5.1 ± 1.2 nmol ATP per oocyte, respectively.
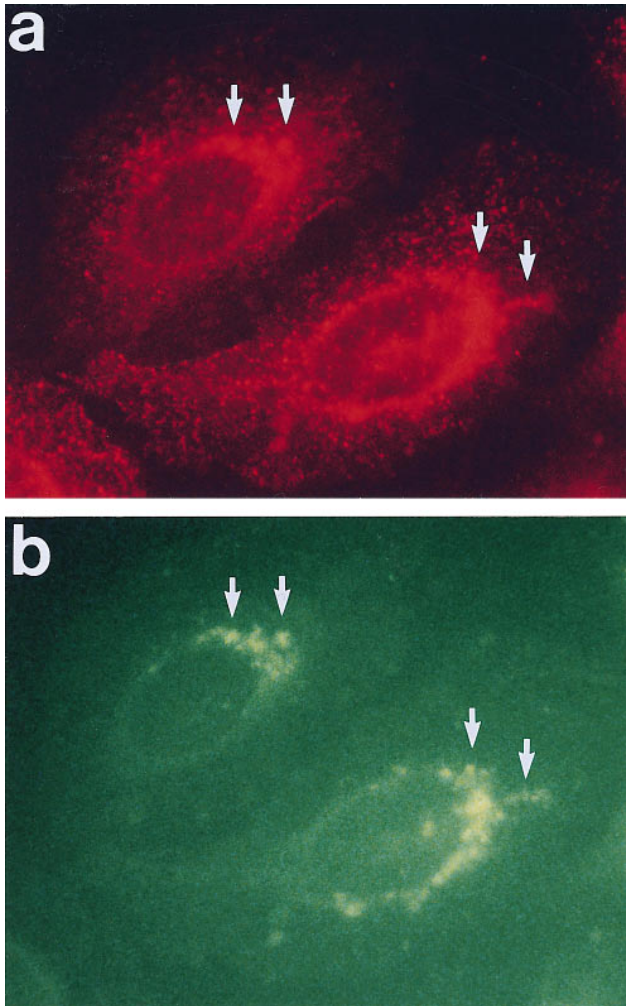
Properties of Fe Uptake Stimulated by SFT

Properties of transport mediated by SFT are summarized in Table I and are quite comparable to known characteristics of the K562 cell, Tf-independent Fe uptake system (Inman and Wessling-Resnick, 1993). Transport by injected oocytes appears to be specific for Fe since uptake was blocked by excess ferric ammonium citrate; this result indicates that the anionic ligand does not influence transmembrane movement of the cation. SFT-mediated uptake is unaffected by the presence of 20 µM Cu, Ni, Co, or Mn (not shown), further demonstrating the specificity of this process. Nonetheless, cadmium, which is a known potent and competitive inhibitor of Tf-independent Fe transport by K562 (Inman and Wessling-Resnick, 1993; Inman et al., 1994) and other cells (Sturrock et al., 1990), also blocks uptake by SFT-injected oocytes (Table I). These data help to verify the authenticity of SFT function in the plasma membrane transport of Fe by mammalian cells.

To examine whether Fe uptake mediated by SFT is an active, energy-requiring process, injected oocytes were treated with antimycin A or rotenone. Both metabolic inhibitors were found to reduce cellular ATP levels to <50% of resting levels and thereby effectively abolish Fe uptake (Table I). Similar observations have been made for K562 cells, confirming that plasma membrane transport of Fe is an energy-consuming process requiring cellular ATP (Gutierrez, J.A., and M. Wessling-Resnick, personal observations).

As noted above, the amino acid sequence REIHE present within the predicted first intracellular loop of SFT appears related to domains important for high affinity Fe transport in yeast (Stearman et al., 1996) and Fe binding by ferritin L chains (Trikha et al., 1995). To evaluate the potential role of this domain in SFT's transport function, the key glutamic acid residues were substituted with alanines by mutagenesis of the SFT-ORF cDNA. The results of oocyte injection experiments shown in Fig. 1 *D* demonstrate that while expression of the SFT-ORF stimulated Fe uptake four- to fivefold above background levels, the E→A mutant failed to produce transport activity above that observed for water-injected oocytes.

SFT Stimulates Fe Uptake from Transferrin

To investigate SFT's function in mammalian cells, a chimera was constructed with GFP fused to its COOH terminus. Fluorescence microscopy experiments were first performed with transiently transfected mammalian cells to

sion of the SFT protein itself is necessary and sufficient to stimulate Fe uptake by *Xenopus* oocytes. These results also reveal the important finding that the untranslated regions of SFT must be involved in some form of posttranscriptional regulation of the protein's expression.
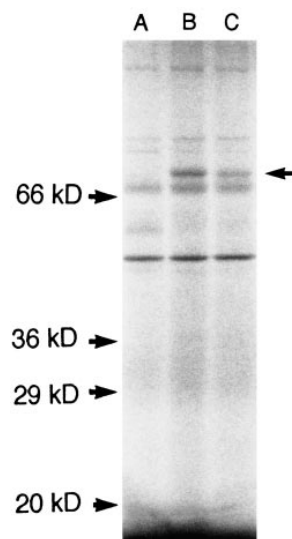
Figure 5. In vitro translation of SFT cRNA in the presence of microsomes. Rabbit reticulocyte lysate was programmed with water (lane *A*), 100 ng SFT-ORF cRNA (lane *B*), or 100 ng full-length SFT cRNA (lane *C*). [35S]Methionine-labeled products were electrophoresed on a 10% SDS–polyacrylamide gel; a fluorograph of the dried gel is shown. SFT is denoted by the right arrow; molecular weight standards (*left*) were bovine serum albumin (*66 kD*), glyceraldehyde 3–phosphate dehydrogenase (*36 kD*), carbonic anhydrase (*29 kD*), and soybean trypsin inhibitor (*20 kD*).

Figure 6. GFP chimera of SFT associates with recycling endosomes. To visualize endocytic compartments, HeLa cells transiently expressing GFP-SFT were incubated with Texas red–Tf as described in Materials and Methods. The upper image is Texas red–Tf fluorescence and overlap with GFP-SFT (*bottom*) is indicated with arrows. To verify that the presence of GFP at SFT's COOH terminus does not interfere with its normal cellular localization, a chimera of SFT with two NH_2-terminal HA tags was also constructed and found to localize to the same domain (not shown).

Figure 7. SFT stimulates assimilation of Fe from Tf. The accumulation of ^{55}Fe from Tf was measured for HeLa cells stably expressing the SFT-GFP chimera (●) as well as control cells (○) as described in Materials and Methods. The amount of cell-associated radioactivity determined for duplicate samples ± SE is shown as a function of time.

SFT with two NH_2-terminal, hemagglutinin (HA)-epitope tags (not shown), suggesting that its cellular membrane distribution is not altered by the addition of the COOH-terminal GFP.

Tf-independent uptake by HeLa cells stably expressing the SFT-GFP chimera was assayed essentially as described above for *Xenopus* oocytes except that incubation was for <10 min at 37°C with 1 μM ^{55}FeNTA. Under these conditions, rates of uptake were measured to be 5.2 ± 0.4 and 11.7 ± 0.7 fmol/μg protein/min for control and SFT-GFP–expressing HeLa cells, respectively ($n = 3$). These results correlate nicely with data obtained for oocytes injected with full-length SFT mRNA, confirming the presence of SFT-GFP at the cell surface and its function in non–Tf-bound Fe transport. Because the intracellular distribution of SFT-GFP indicated that it might play an additional role in Tf-mediated delivery by transporting Fe released in endosomal compartments, assimilation from [^{55}Fe]Tf was also measured. As shown in Fig. 7, the accumulation of ^{55}Fe from 40 nM Tf is linear with time; for HeLa cells expressing SFT-GFP, the rate of Fe assimilation is enhanced (Fig. 7, ●). In a series of similar experiments, the rate of ^{55}Fe assimilation from Tf by HeLa cells expressing SFT-GFP was found be increased 65 ± 11% ($n = 3$). Iron accumulation was blocked by excess unlabeled Tf and was inhibited by 50 μM chloroquine (not shown). Assuming that the presence of GFP does not alter the activity of the chimera, these combined results are consistent with the idea that SFT also functions in the import of Tf-bound iron, acting as a true physiological stimulator of Fe transport.

SFT Contains a 3′ Untranslated Region (UTR) Element Related to TIE

As noted above, the fact that the elimination of 5′ and 3′ untranslated regions of the full-length SFT message enables functional expression of Fe uptake activity indicates some form of posttranscriptional regulation. It is unlikely that message stability is affected since SFT expression can be supported by coinjection of other defined cRNAs (Fig. 1 *B*). In searching for known translational control elements, a sequence within SFT's 3′ UTR was found to have striking homology with a *cis*-acting element involved in developmental expression of the XFGFR-1, TIE (Robbie et al., 1995). As shown in Table II, a 41-base stretch within SFT's UTR displays 65.8% identity and 78% similarity to a sequence present within the 180-nucleotide region known to contain the XFGFR's TIE.

Transcripts for XFGFR are stored as untranslated ma-

determine which cellular compartments harbor SFT-GFP. As shown in Fig. 6, Texas red–Tf internalized by HeLa cells is located in small, punctate peripheral sorting endosomes and is highly concentrated in a juxtanuclear region referred to as a recycling compartment (Dunn et al., 1989). The latter is a post-sorting endocytic compartment that contains recycling Tf receptors, but not internalized LDL. The GFP chimera of SFT is also found to be concentrated within this compartment, as indicated by arrows (Fig. 6). Some rather minor and diffuse staining is observed at the cell's plasmalemma, suggesting that like many membrane proteins, SFT may traffic between the cell surface and endocytic compartments. However, at steady-state, GFP-SFT appears to be concentrated primarily in recycling endosomes rather than peripheral sorting endosomes and/or the plasma membrane. Similar results were obtained for

Table II. Homologies between TIE and 3′ UTR Elements

```
G U U C U U C U C C A U A A A U U C C A U U U A A A G A A C A U U U G U U U U G A   TIE
G U A A U U C U C A G C A T A C U G A U U A U G G A G A A C A C U U U G U U U U G A   SFT


A G A A C A U U U G U U U U G A      TIE (3'UTR Xenopus FGF receptor-1)
A G A A C A C U U U G U U U U G A    SFT (3'UTR Stimulator of Fe Transport)
A G A A C A U U U G U C A G G C      clone 1400 (predicted 3'UTR)
U G C A C A U U G C U U U C C        clone 1900 (predicted 3'UTR)
A G A A A A U A U U G U A G U A      ACADM (3'UTR Acyl-CoA Dehydrogenase)
C C A A G A U U G C U C U U U U      HSP70 (3'UTR Heat Shock Protein)

A G A A C A U U U G U U U U G A      Consensus
```

ternal mRNA in immature oocytes and become translationally active upon meiotic maturation (Musci et al., 1990). However, synthetic transcripts lacking the XFGFR 3′ UTR yield expressed product when injected into immature oocytes (Robbie et al., 1995); this phenomenon correlates with the observed pattern of SFT expression in immature oocytes injected with the ORF versus full-length cRNA (Fig. 1 B). Whereas exogenous XFGFR transcripts containing the TIE are not translated, XFGFR is synthesized when the injected oocytes are induced to mature in vitro by progesterone treatment (Robbie et al., 1995). Therefore, to verify whether a similar translational control mechanism is exerted through the untranslated regions of SFT, Fe uptake activity was measured for progesterone-treated oocytes microinjected with the full-length cRNA (Fig. 8). Whereas progesterone treatment itself appears to limit the overall extent of SFT-mediated uptake, ^{55}Fe transport activity is quite comparable to progesterone-treated cells injected with SFT-ORF cRNAs (Fig. 8, compare solid bars). Thus, very much like the maternal XF-GFR message, full-length SFT transcript contains a TIE such that protein synthesis is blocked in immature oocytes. The idea that the 41-base elements noted in Table II are related is strongly supported by preliminary observations that a ∼43-kD *Xenopus* oocyte protein that cross-links to the 180-nucleotide XFGFR TIE element (Robbie et al., 1995) also binds to the 3′ UTR of SFT (T. Musci, personal communication).

Characterization of Clones Enabling Fe Transport When Coinjected with Full-length SFT

As indicated earlier, four unique clones were found to enable functional transport activity when their transcripts are coinjected into immature oocytes with full-length SFT message. Sequence analysis revealed that the smallest clone, a ∼650-bp cDNA, has 100% identity with nucleotides 1,395–2,019 of human medium chain acyl co-A de-
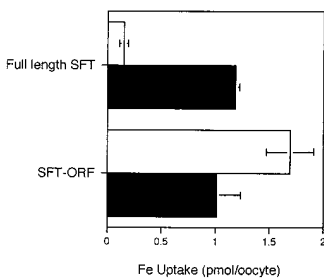

Figure 8. Meiotic maturation of oocytes with progesterone promotes expression of SFT activity. Fe transport was measured as in Fig. 1 except that some oocytes were treated with 1 μM progesterone 24 h after injection (*solid bars*). Transport of ^{55}Fe was normalized by subtracting measurements made for water-injected oocytes for each condition. Shown are results from a single experiment and are representative of those obtained on three separate occasions; data are the average values ± SE (n = 15 oocytes).

hydrogenase (ACADM; these sequence data are available from GenBank/EMBL/DDBJ under accession number M16827 J05355). Surprisingly, this noncoding sequence falls within the predicted 3′ UTR of the ACADM message. Moreover, the ∼1,000-bp cDNA was found to have 100% identity with nucleotides 1,800–2,691 of human heat shock protein (HSP70; these sequence data are available from GenBank/EMBL/DDBJ under accession number M11717 M15432), encoding only a small fragment of this protein's COOH terminus but with all of the known 3′ UTR of its message represented. The two larger cDNAs encode as yet unidentified factors. The ∼1,400-bp clone contains a partial ORF; the 267 amino acids of this hypothetical protein reveal some relationship to YOL010c, a probable membrane protein of unknown function in *Saccharomyces cerevisiae* (Vandenbol et al., 1995). Notably, 514 nucleotides of this cDNA represent a predicted 3′ untranslated region (these sequence data are available from GenBank/EMBL/DDBJ under accession number AF020762). The ∼1,900-bp cDNA appears to encode a single complete ORF (GenBank/EMBL/DDBJ accession number AF020763). Its predicted translation product hypothetically would be a small soluble factor, but a functional relationship with known human gene products is not obvious. Nonetheless, this clone also harbors a predicted 226-nucleotide 3′ UTR element.

The only common feature readily discerned for these four *trans*-acting clones is that their transcripts provide 3′ untranslated sequences. The fact that the 650-bp clone is from the noncoding 3′ UTR of ACADM indicates that its transcript in particular must function at the RNA level. Moreover, since all four clones are unique, it is highly unlikely that their transcripts provide a common protein function required for expression of SFT-mediated transport. Given that SFT's untranslated region must contain a posttranscriptional control element inhibiting functional expression in the immature oocyte, an attractive hypothesis is that the complementing clones provide UTR sequences that compete in *trans* to alleviate the translational block. Indeed, within the 41-base region of SFT's homology with TIE, a highly conserved 16-base element is found in the 3′ UTRs these other clones (Table II). Whereas this element is not as well conserved in all of the cDNAs, the most remote sequence found in HSP70's 3′ UTR has overall 50% identity but 75% similarity. Table III summarizes the probability of finding the consensus 16-base segment within these UTRs. Whereas the probability that the match for the 16-base 3′ UTR sequence for ACADM and HSP70 occurs by random chance is high, it is unlikely that the match for the ∼1,400- and ∼1,900-bp clones is simply coincidental. Moreover, ACADM and HSP70 are the two complementing cDNAs that predominantly contain noncoding 3′ sequences, supporting a function for these untranslated elements at the RNA level. Finally, the chance of simultaneously finding five 16-base UTR elements with identity as or more related to that observed (Table III) is calculated to be <0.1%, thus the global significance of these results strongly suggests that a biological link resides in this domain.

Discussion

The molecular cloning of SFT through expression in *Xe-*

Table III. Relationship between 16-base Consensus Elements

cDNA	UTR length	Observed identity	*P*-value
		r	
SFT	279	15	3.0×10^{-6}
c1400	514	12	0.067
c1900	226	10	0.107
ACADH	650	9	>0.999
HSP70	281	8	>0.999

Exact *P* values that the number of matches >*r* would be found within a 16-base segment of a UTR region of length *n* were calculated from a binomial probability function. The probability of finding matches as or more extreme as those observed simultaneously for all five clones was calculated by the inverse chi-square method of combining *P* values to test global significance and found to have a highly significant *P* value of ~0.0001.

nopus oocytes was accomplished using a Latin square experimental design; this approach identified two sets of clones that when coinjected, provided functional Fe uptake. To our knowledge, this is the first example of the use of such a strategy to screen for the activity of multiple factors by injection into oocytes and in theory, multi-subunit complexes could be isolated using this double-grouping technique. However, the discovery of SFT was unexpectedly coupled to the revelation of a translational control element in the untranslated regions of its cRNA. Because additional accessory cRNAs were first found to be required for Fe transport activity by oocytes injected with full-length SFT transcripts, this novel factor was called a stimulator of Fe transport. The fact that deletion of SFT's untranslated regions enables expression of transport activity in the absence of other factors, along with SFT's structural and functional characteristics, indicates that it is a strong candidate to be the actual membrane Fe carrier.

Although database searches reveal little homology with yeast (Dix et al., 1994; Stearman et al., 1996), plant (Eide et al., 1996), and bacterial (Kammler et al., 1982) Fe transporters, all of these proteins and SFT are of similar size (~40–70 kD) and secondary structure with either six or eight predicted membranous domains. Moreover, alanine substitutions for the critical glutamic acid residues of SFT's RExxE motif specifically eliminate transport; identical mutations in the cognate domain of the yeast Ftr1 transporter also disable Fe uptake (Stearman et al., 1996). However, whereas this domain is hypothesized to reside in the first intracellular loop of SFT, it falls within a membranous domain predicted for Ftr1. The structural context of this domain may reflect mechanistic differences between these two molecules, and indeed, attempts to complement a yeast FTR1 deletion mutant with SFT have thus far proven unsuccessful (Yu, J., and M. Wessling-Resnick, personal observations). The latter finding is not unexpected particularly since the *Schizosaccharomyces pombe* homologue, Fip1, also is unable to complement defects in *S. cerevisiae* FTR1 mutants unless coexpressed with the *S. pombe* Fet3 multicopper oxidase homologue Fio1 (Askwith and Kaplan, 1997). The role of such a membrane-associated oxidase activity in SFT-mediated transport has yet to be discerned. Thus, although our results demonstrate the functional importance of the RExxE motif in close analogy to the Ftr1 domain, experiments to determine the actual disposition of SFT and Ftr1 within the membrane bi-

layer will help to better define the mechanistic attributes of this site.

It is also noteworthy that SFT displays no structural or functional homology with the family of Nramp transporters recently identified as H^+-coupled metal ion transporters mediating the uptake of multiple divalent cations including Fe^{2+} (Gunshin et al., 1997). Fleming et al. (1997) have reported that *mk* mice, which have microcytic anemia due to apparent defects in iron absorption and use, display a missense mutation in Nramp2. However, the relationship between Nramp transporters and SFT, and their respective roles in the absorption of dietary iron remains to be more fully clarified. Functionally, transport activity by oocytes injected with the SFT-ORF cRNA has properties very much related to those characterized for Tf-independent Fe uptake by K562 cells (Inman and Wessling-Resnick, 1993; Inman et al., 1994). Unlike the Nramp transporter DCT1 (Gunshin et al., 1997), SFT-mediated uptake is specific for Fe since other transition metals fail to compete for transport. The one exception is the observed sensitivity to cadmium that has been reported also to inhibit Fe transport by HeLa cells (Sturrock et al., 1990) as well as K562 cells (Inman and Wessling-Resnick, 1993). Moreover, the transport of Fe stimulated by SFT is energy dependent, which is in agreement with results obtained for non–Tf-bound Fe uptake by K562 cells (Gutierrez, J.A., and M. Wessling-Resnick, personal observations). Finally, the fact that PMA enhances the level of SFT mRNA in K562 cells further confirms its relationship to the latter transport system that is subject to transcriptional regulation (Akompong et al., 1995). All of these independent lines of evidence provide strong support for the candidacy of SFT as a membrane Fe transporter.

The observation that SFT oligomerizes even in the presence of 2.5% β-mercaptoethanol and 1% SDS prompts the notion that this putative transport protein may be a member of the ATP-binding cassette (ABC) transporter family, which is known to maintain its oligomeric assembly upon SDS-PAGE. The ABC family of carriers couple the hydrolysis of ATP to the uptake of a variety of substrates including inorganic ions (Higgins, 1992). A common structural paradigm for these carriers is the homo- or heterooligomerization of two six-transmembrane spanning domain subunits that function in association with two soluble ATP-binding components. Interestingly, the bacterial Fe carrier FeoB is a well-characterized member of this transporter class (Kammler et al., 1993); functional mechanisms associated with the yeast Ftr1 and Fet4 transporters have not been determined. The fact that SFT-mediated oocyte Fe uptake requires cellular ATP provides support for the idea that this protein may be an ABC family member, although SFT does not contain the so-called Walker motifs, commonly present in oligomeric ABC carrier assemblies (Higgins, 1992). Thus, a caveat to this hypothesis is that endogenous oocyte factors must provide the ABC domains to enable the vectorial coupling of ATP hydrolysis with SFT-mediated transport.

Another strong possibility is that SFT and other six-transmembrane spanning domain metal cation transporters represent a novel class of membrane proteins with a yet to be defined transport mechanism. Recent reports have suggested that several heavy metal ion transport pro-

teins may be related as members of the cation diffusion facilitator (CDF) family (Nies and Silver, 1995). Paulsen and Saier (1997) have identified 13 members of this class with representatives found in both prokaryotes and eukaryotes. All CDF family members appear to possess six putative transmembrane spanning domains; however, although this characteristic is fulfilled by SFT's predicted secondary structure, its primary sequence lacks a signature motif that has been derived for CDF family members (Paulsen and Saier, 1997). The relationship of CDF and ABC family members also remains to be fully clarified. Nonetheless, it is important to note that like SFT, members of both families that are known to transport heavy metals in eukaryotic cells, are found within intracellular organelles (Conklin et al., 1992; Ortiz et al., 1992; Conklin et al., 1994; Palmiter et al., 1996).

Whereas SFT's structural and functional features provide some hints regarding possible transport mechanisms, whether or not additional factors provided by the oocyte are involved in facilitating Fe uptake remains to be determined. It should be emphasized that although all of these characteristics are consistent with the hypothesis that SFT is a true membrane carrier for iron, rigorous evidence is still lacking. The apparent stimulation of oocyte Fe transport upon injection of SFT transcripts could be explained by the activation of an endogenous uptake system. This important caveat is fully recognized when one carefully considers new roles attributed to ABC family members that may regulate or activate membrane channels, serve as intracellular channels, or possibly regulate intracellular vesicular traffic (Higgins, 1995).

A critical finding that does support a direct role for SFT in Fe membrane transport is that the protein does not exclusively stimulate Tf-independent, cell surface uptake. Its cytolocalization and ability to stimulate the uptake of Tf-bound Fe in mammalian cells suggests a key role in intracellular Fe transport as well. The predominant localization of the GFP chimera within endosomal compartments supports the idea that SFT's major function may actually be the acquisition of Tf-bound Fe; this notion is consistent with the relationship between Tf-independent and -dependent activity in K562 cells since the latter is $\sim$10-fold more effective in Fe assimilation (Inman and Wessling-Resnick, 1993). Like many other membrane proteins, SFT appears to traffic between the cell surface and intracellular compartments, but it is predominantly localized to recycling endosomes rather than peripheral sorting endosomes, which are the first acidic compartment encountered by internalized Tf. The differences in the intracellular distribution of Tf receptors and SFT may be an indication that the latter is more efficiently targeted to recycling endosomes and/or less efficiently trafficked out of the recycling endosome. The apparent steady-state distribution of SFT does not rule out the possibility that it functions to transport Fe across the membrane of peripheral sorting endosomes, thus, exactly where SFT acts to stimulate the transport of Fe released from Tf remains unknown. Moreover, the expression of SFT-GFP could only stimulate this process if SFT is normally present in rate-limiting amounts. Further work is required to verify that expression of transfected SFT is sufficient to account for the observed increase in both Tf-dependent and -independent Fe uptake. Until a more precise determination can be made of SFT's true function, the name, stimulator of Fe transport, seems most appropriate particularly in view of its ability to enhance the assimilation of Tf-bound Fe.

The relationship between the four unique cDNAs that complement transport activity expressed by full-length SFT also requires further elucidation. It is clear that the 41-base element in SFT's 3′ UTR is highly related to the *cis*-acting TIE of the XFGFR, both at the molecular and functional level. Our working hypothesis is that these *trans*-acting factors act at the RNA level to compete for association with TIE-binding protein thereby releasing a translational block on SFT expression, but other mechanisms by which these factors promote its function in the immature oocyte are equally plausible. One experimental test of this model will be to determine if XGFGR expression can be initiated by injection of oocytes with the complementing cRNAs and investigation is currently underway to functionally characterize these *trans*-acting factors. Why does a translational silencing element appear in the 3′ untranslated region of SFT? A simple explanation is that the homologous TIE was found by the choice of cloning vehicle: immature oocytes that repress translation of maternal mRNA. The Latin square approach therefore enabled the identification of SFT's activity that would otherwise have gone undetected. Evidence that this 3′ UTR element functions in mammalian cells is still lacking, but it is quite possible that SFT's translational inhibitory element represents a more universal mechanism for coordinated posttranscriptional regulation that future studies may yet reveal.

References

Akompong, T., R.S. Inman, and M. Wessling-Resnick. 1995. Phorbol esters stimulate non-transferrin iron uptake by K562 cells. *J. Biol. Chem.* 270:20937–20941.

Askwith, C., D. Eide, A.V. Ho, P.S. Bernard, L. Li, S. Davis-Kaplan, D.M. Sipe, and J. Kaplan. 1994. The FET3 gene of *S. cerevisiae* encodes a multi-copper oxidase required for ferrous iron uptake. *Cell.* 67:403–410.

Askwith, C., and J. Kaplan. 1997. An oxidase-permease-based iron transport system in *Schizosaccharomyces pombe* and its expression in *Saccharomyces cerevisiae. J. Biol. Chem.* 272:401–405.

Birnboim, H.C., and J. Dolly. 1979. A rapid alkaline extraction procedure for screening recombinant plasmid DNA. *Nucleic Acid Res.* 7:1513–1524.

Conklin, D.S., J.A. McMaster, M.R. Culbertson, and C. Kung. 1992. COT1, a gene involved in cobalt accumulation in *Saccharomyces cerevisiae. Mol. Cell. Biol.* 12:3678–3688.

Conklin, D.S., M.R. Culbertson, and C. Kung. 1994. Interactions between gene products involved in divalent cation transport in *Saccharomyces cerevisiae. Mol. Gen. Genet.* 244:303–311.

Dancis, A., D.G. Roman, G.J. Anderson, A.G. Hinnebusch, and R.D. Klausner. 1992. Ferric reductase of *Saccharomyces cerevisiae*: molecular characterization, role of iron uptake, and transcriptional control by iron. *Proc. Natl. Acad. Sci. USA.* 89:3869–3973.

Dautry-Varsat, A., A. Ciechanover, and H.F. Lodish. 1983. pH and the recycling of transferrin during receptor-mediated endocytosis. *Proc. Natl. Acad. Sci. USA.* 80:2258–2262.

De Silva, D.M., C.C. Askwith, D. Eide, and J. Kaplan. 1995. The FET3 gene product required for high-affinity iron transport in yeast is a cell surface ferroxidase. *J. Biol. Chem.* 270:1098–1101.

Dix, D.R., J.T. Bridgham, M.A. Broderius, C.A. Byersdorfer, and D.J. Eide. 1994. The FET4 gene encodes the low-affinity Fe(II) transport protein of *Saccharomyces cerevisiae*. *J. Biol. Chem.* 269:26092–26099.

Dunn, K.W., T.E. McGraw, and F.R. Maxfield. 1989. Iterative fractionation of recycling receptors from lysosomally destined ligands in an early sorting endosome. *J. Cell Biol.* 109:3303–3314.

Eide, D., M. Broderius, J. Fett, and M.L. Guerinot. 1996. A novel iron-regulated metal transporter from plants identified by functional expression in yeast. *Proc. Natl. Acad. Sci. USA.* 93:5624–5628.

Fleming, M.D., C.C. Trenor III, M.A. Su, D. Foernzler, D.R. Beier, W.F. Dietrich, and N.C. Andrews. 1997. Microcytic anaemia mice have a mutation in Nramp2, a candidate iron transporter gene. *Nat. Genet.* 16:383–386.

Gubler, V., and R.J. Hoffman. 1983. A simple and very efficient method for generating cDNA libraries. *Gene (Amst.).* 25:255–263.

Gunshin, H., B. Mackenzie, U.V. Berger, Y. Gunshin, M.R. Romero, W.F. Boron, S. Nussberger, J.L. Gollan, and M.A. Hediger. 1997. Cloning and characterization of a mammalian proton-coupled metal-ion transporter. *Nature.* 388:482–487.

Hanahan, D. 1983. Studies on the transformation of *E. coli* with plasmids. *J. Mol. Biol.* 166:557–580.

Higgins, C.F. 1992. ABC transporters: from microorganisms to man. *Annu. Rev. Cell Biol.* 8:67–113.

Higgins, C.F. 1995. The ABC of channel regulation. *Cell.* 82:693–696.

Inman, R.S., and M. Wessling-Resnick. 1993. Characterization of transferrin-independent iron transport in K562 cells: unique properties provide evidence for multiple pathways of iron uptake. *J. Biol. Chem.* 268:8521–8528.

Inman, R.S., M.M. Coughlan, and M. Wessling-Resnick. 1994. Extracellular ferrireductase activity in K562 cells is coupled to transferrin-independent transport. *Biochemistry.* 33:11850–11857.

Jordan, I., and J. Kaplan. 1994. The mammalian transferrin-independent iron transport system may involve a surface ferrireductase activity. *Biochem. J.* 302:875–879.

Kammler, M., C. Schon, and K. Hantke. 1993. Characterization of the ferrous iron uptake system of *Escherichia coli*. *J. Bacterol.* 175:6212–6219.

Klausner, R.D., J.V. Ashwell, J.B. Van Renswoude, J. Harford, and K. Bridges. 1983. Binding of apotransferrin to K562 cell: explanation of the transferrin cycle. *Proc. Natl. Acad. Sci. USA.* 80:2263–2266.

Klausner, R.D., T.A. Roualt, and J.B. Harford. 1993. Regulating the fate of mRNA: the control of cellular iron metabolism. *Cell.* 72:19–28.

Kyte, J., and R.F. Doolittle. 1982. A simple method for displaying the hydropathic character of a protein. *J. Mol. Biol.* 157:105–132.

Masu, Y., K. Nakayama, H. Tamaki, Y. Harada, M. Kuno, and S. Nakanishi. 1987. cDNA cloning of bovine substance-K receptor through oocyte expression system. *Nature.* 329:836–838.

Melton, D.A., P.A. Kreig, T. Rebagliati, K. Maniatis, K. Zinn, and M.R. Green. 1984. Efficient in vitro synthesis of biologically active RNA and RNA hybridization probes from plasmids containing a bacteriophage SP6 promoter. *Nucleic Acids Res.* 12:7035–7056.

Musci, T.J., E. Amaya, and M.W. Kirschner. 1990. Regulation of the fibroblast growth factor receptor in early *Xenopus* embryos. *Proc. Natl. Acad. Sci. USA.* 87:8365–8369.

Nies, D.H., and S. Silver. 1995. Ion efflux systems involved in bacterial metal resistances. *J. Ind. Microbiol.* 14:186–199.

Nomizu, T., K.H. Falchuk, and B.L. Vallee. 1993. Zinc, iron, and copper contents of *Xenopus laevis* oocytes and embryos. *Mol. Reprod. Dev.* 36:419–423.

Nunez, M.T., V. Gaete, J.A. Watkins, and J. Glass. 1990. Mobilization of iron from endocytic vesicles, the effects of acidification and reduction. *J. Biol. Chem.* 265:6688–6692.

Ortiz, D.F., L. Kreppel, D.M. Speiser, G. Scheel, G. McDonald, and D.W. Ow. 1992. Heavy metal tolerance in the fission yeast requires an ATP-binding cassette-type vacuolar membrane transporter. *EMBO (Eur. Mol. Biol. Organ.) J.* 11:3491–3499.

Oshiro, S., H. Nakajima, T. Markello, D. Krasnewick, I. Bernardini, and W.A. Gahl. 1993. Redox, transferrin-independent, and receptor-mediated endocytosis iron uptake systems in cultured human fibroblasts. *J. Biol. Chem.* 268:21586–21591.

Palmiter, R.D., T.B. Cole, and S.D. Findley. 1996. ZnT-2, a mammalian protein that confers resistance to zinc by facilitating vesicular sequestration. *EMBO (Eur. Mol. Biol. Organ.) J.* 15:1784–1791.

Paulsen, I.T., and M.H. Saier, Jr. 1997. A novel family of ubiquitous heavy metal ion transport proteins. *J. Membr. Biol.* 156:99–103.

Randell, E.W., J.G. Parkes, N.F. Olivieri, and D.M. Templeton. 1994. Uptake of non-transferrin-bound iron by both reductive and nonreductive processes is modulated by intracellular iron. *J. Biol. Chem.* 269:16046–16053.

Riedel, H.-D., A.J. Remus, B.A. Fitscher, and W. Stremmel. 1995. Characterization and partial purification of a ferrireductase from human duodenal microvillus membranes. *Biochem. J.* 309:745–748.

Robbie, E.P., M. Peterson, E. Amaya, and T.J. Musci. 1995. Temporal regulation of the Xenopus FGF receptor in development: a translation inhibitory element in the 3′ untranslated region. *Development (Cambr.).* 21:1775–1785.

Sanford, J., J. Codina, and L. Birnbaumer. 1991. γ-subunits of G proteins, but not their α- or β-subunits, are polyisoprenylated. *J. Biol. Chem.* 266:9570–9579.

Stearman, R., D.S. Yuan, Y. Yamaguchi-Iwai, R.D. Klausner, and A. Dancis. 1996. A permease-oxidase complex involved in high-affinity iron uptake in yeast. *Science.* 271:1552–1557.

Steel, R.G.D., and J.H. Torrie. 1980. Principles and Procedures of Statistics. McGraw-Hill, New York. 221–229.

Sturrock, A., J. Alexander, J. Lamb, C.M. Craven, and J. Kaplan. 1990. Characterization of a transferrin-independent uptake system for iron in HeLa cells. *J. Biol. Chem.* 265:3139–3145.

Trikha, J., E.C. Theil, and N.M. Allewell. 1995. High resolution crystal structures of amphibian red-cell L ferritin: potential roles for structural plasticity and solvation in function. *J. Mol. Biol.* 248:949–967.

Vandenbol, M., P. Durand, D. Portetelle, and F. Hilger. 1995. Sequence analysis of a 44 kb DNA fragment of yeast chromosome XV including the Ty1-H3 retrotransposon, the suf1(+) frameshift suppressor gene for tRNA-Gly, the yeast transfer RNA-Thr-1a and a Delta element. *Yeast.* 11:1069–1075.

Von Heijne, G. 1994. Membrane proteins: from sequence to structure. *Annu. Rev. Biophys. Biomol. Struct.* 23:167–192.

Watkins, J.A., J.D. Altazan, P. Elder, C.Y. Li, M.T. Nunez, X.X. Cui, and J. Glass. 1992. Kinetic characterization of reductant-dependent processes of iron mobilization from endocytic vesicles. *Biochemistry.* 31:5820–5830.